Nonlinear Analysis of Composite Laminates Using a Generalized Laminated Plate Theory

E. J. Barbero*
West Virginia University, Morgantown, West Virginia 26506
and
J. N. Reddy†
Virginia Polytechnic Institute and State University, Blacksburg, Virginia 24061

The nonlinear version of the generalized laminated plate theory of Reddy is presented, and it is used to investigate nonlinear effects in composite laminates. A plate-bending finite element based on the theory is developed, and its accuracy is investigated by comparison with exact and approximate solutions to conventional plate theories. The element has improved description of the in-plane as well as the transverse deformation response. The theory is further applied to study various aspects of the geometrically nonlinear analysis of composite plates. It is shown that inclusion of the geometric nonlinearity relaxes stress distributions and that composite laminates with bending-extensional coupling do not exhibit any bifurcation (i.e., no apparent critical buckling load exists).

Introduction

LAMINATED composite plates are relatively weak in shear compared to their metallic counterparts because of their low transverse shear moduli. The single-layer classical and shear deformation theories based on a continuous displacement field through thickness are adequate for predicting global response characteristics, such as maximum deflections stresses and fundamental natural frequencies. The first-order and higher-order shear deformation theories[1] yield improved global response over the classical laminate theory because the former account for transverse shear strains. Both classical and refined plate theories based on a single continuous displacement field through thickness give poor estimation of interlaminar stresses. The fact that some important modes of failure are related to interlaminar stresses motivated researchers to search for refined plate theories that can model the layer-wise kinematics appropriately and predict interlaminar stresses accurately.[2-5] For example, a study of localized damage (e.g., delaminations) requires a more precise representation of the laminate deformation than that allowed by the equivalent single-layer laminate theories.

The generalized laminate theory proposed by Reddy[2] and advanced by him and his colleagues[5,7] allows layer-wise representation of the displacement field and results in an accurate determination of stresses. With the choice of linear approximation of the in-plane displacements through the thickness of each layer, continuous interlaminar stresses can be recovered.[5-7] Analytical solutions of the linear theory were developed for plates[5] and cylindrical shells[7] to evaluate the accuracy of the theory compared to the three-dimensional elasticity theory. The results indicated that the generalized laminate plate theory allows accurate determination of interlaminar stresses. Furthermore, this theory provides a detailed description of the laminated nature of the plate, adequate for the study of localized damage.

The present study is an extension of Reddy's theory[2] to include geometric nonlinearity, to develop its nonlinear finite element model, and to utilize the model to investigate the effects of geometric nonlinearity on stresses and load-deflection behavior of composite laminates. The finite element model developed herein accounts for the von Kármán nonlinear strains. A series of numerical examples are presented that provide insight into certain interesting behavior of laminated composite plates. Stress relaxation and stiffening of transversely loaded laminates during nonlinear bending is demonstrated. The usefulness of bifurcation analysis in compressively loaded asymmetric laminates is investigated.

Received May 19, 1989; revision received Dec. 5, 1989; accepted for publication Dec. 12, 1989.

*Clifton C. Garvin Professor, Mechanical and Aerospace Engineering Department.

†Assistant Professor, Engineering Science and Mechanics Department.

Formulation of the Theory

Displacements and Strains

The displacements (u_1,u_2,u_3) at a point (x,y,z) in the laminate are assumed to be of the form[2]

$$u_1(x,y,z) = u(x,y) + U(x,y,z)$$

$$u_2(x,y,z) = v(x,y) + V(x,y,z)$$

$$u_3(x,y,z) = w(x,y) \tag{1}$$

where (u,v,w) are the displacements of a point $(x,y,0)$ on the reference plane of the laminate, and U and V are functions that vanish on the reference plane:

$$U(x,y,0) = V(x,y,0) = 0 \tag{2}$$

The displacement field in Eq. (1) forms the basis of the present theory.

The von Kármán strains associated with the displacements in Eq. (1) are given by

$$\epsilon_x = \frac{\partial u}{\partial x} + \frac{\partial U}{\partial x} + \frac{1}{2}\left(\frac{\partial w}{\partial x}\right)^2, \qquad \epsilon_y = \frac{\partial v}{\partial y} + \frac{\partial V}{\partial y} + \frac{1}{2}\left(\frac{\partial w}{\partial y}\right)^2$$

$$2\epsilon_{xy} = \left(\frac{\partial u}{\partial y} + \frac{\partial v}{\partial x}\right) + \left(\frac{\partial U}{\partial y} + \frac{\partial V}{\partial x}\right) + \frac{\partial w}{\partial x}\frac{\partial w}{\partial y} \tag{3}$$

$$2\epsilon_{xz} = \frac{\partial U}{\partial z} + \frac{\partial w}{\partial x}, \qquad 2\epsilon_{yz} = \frac{\partial V}{\partial z} + \frac{\partial w}{\partial y}$$

The principle of virtual displacements is used to derive a consistent set of differential equations governing the equi-

librium of a laminate composed of N constant-thickness orthotropic lamina; the material axes of each lamina are arbitrarily oriented with respect to the laminate coordinates.

Thickness Approximation

In order to reduce the three-dimensional theory to a two-dimensional theory, it is necessary to make an assumption concerning the variation of U and V with respect to the thickness coordinate z. To keep the flexibility of the degree of variation of the displacements through thickness, we assume that U and V are approximated as

$$U(x,y,z) = \sum_{j=1}^{n} u^j(x,y)\Phi_j(z) \tag{4a}$$

$$V(x,y,z) = \sum_{j=1}^{n} v^j(x,y)\Phi_j(z) \tag{4b}$$

where u^j and v^j are undetermined coefficients and Φ_j are any continuous functions that satisfy the condition

$$\Phi_j(0) = 0 \text{ for all } j = 1,2,\ldots, n \tag{5}$$

The approximation in Eqs. (4) can also be viewed as the global semidiscrete finite element approximations of U and V through thickness. In that case, Φ_j denotes the global interpolation functions, and u^j and v^j are the nodal values of U and V at the nodes through the thickness of the laminate. A number of other well-known theories can be obtained from the present theory.[1,2,9]

Governing Equations

The nonlinear equations relating u, v, w, u^j, and v^j can be derived using the virtual work principle. Substituting Eqs. (4) into the virtual work principle (see Ref. 1), we obtain the weak (or variational) statement of the present theory,

$$\begin{aligned} 0 = \int_\Omega \Bigg\{ & N_x\left(\frac{\partial \delta u}{\partial x} + \frac{\partial w}{\partial x}\frac{\partial \delta w}{\partial x}\right) + N_y\left(\frac{\partial \delta v}{\partial y} + \frac{\partial w}{\partial y}\frac{\partial \delta w}{\partial y}\right) + N_{xy} \\ & \times \left(\frac{\partial \delta u}{\partial y} + \frac{\partial \delta v}{\partial x} + \frac{\partial w}{\partial x}\frac{\partial \delta w}{\partial y} + \frac{\partial \delta w}{\partial x}\frac{\partial w}{\partial y}\right) + Q_x\frac{\partial \delta w}{\partial x} + Q_y\frac{\partial \delta w}{\partial y} \\ & + \sum_{j=1}^{n}\Bigg[N_x^j\frac{\partial \delta u^j}{\partial x} + N_y^j\frac{\partial \delta v^j}{\partial y} + N_{xy}^j\left(\frac{\partial \delta u^j}{\partial y} + \frac{\partial \delta v^j}{\partial x}\right) \\ & + Q_x^j u^j + Q_y^j v^j\Bigg] - p\,\delta w\Bigg\}\, dA \end{aligned} \tag{6a}$$

where p is the distributed transverse load, and

$$\begin{aligned} (N_x,N_y,N_{xy}) &= \int_{-h/2}^{h/2} (\sigma_x,\sigma_y,\sigma_{xy})\, dz \\ (Q_x,Q_y) &= \int_{-h/2}^{h/2} (\sigma_{xz},\sigma_{yz})\, dz \\ (N_x^j,N_y^j,N_{xy}^j) &= \int_{-h/2}^{h/2} (\sigma_x,\sigma_y,\sigma_{xy})\Phi_j(z)\, dz \\ (Q_x^j,Q_y^j) &= \int_{-h/2}^{h/2} (\sigma_{xz},\sigma_{yz})\frac{d\Phi_j}{dz}(z)\, dz \end{aligned} \tag{6b}$$

The Euler-Lagrange equations of the theory are

$$\begin{aligned} N_{x,x} + N_{xy,y} &= 0 \\ N_{xy,x} + N_{y,y} &= 0 \\ Q_{x,x} + Q_{y,y} + N(w) + p &= 0 \\ N_{x,x}^j + N_{xy,y}^j - Q_x^j &= 0 \\ N_{xy,x}^j + N_{y,y}^j - Q_y^j &= 0; \quad j = 1,2,\ldots, n \end{aligned} \tag{7a}$$

where $N(w)$ is due to the inclusion of the von Kármán nonlinearity in the theory

$$N(w) = \frac{\partial}{\partial x}\left(N_x\frac{\partial w}{\partial x} + N_{xy}\frac{\partial w}{\partial y}\right) + \frac{\partial}{\partial y}\left(N_{xy}\frac{\partial w}{\partial x} + N_y\frac{\partial w}{\partial y}\right) \tag{7b}$$

There are $(2n + 3)$ differential equations in $(2n + 3)$ variables (u,v,w,u^j,v^j). The form of the geometric and force boundary conditions is given below

Geometric (essential)	Force (natural)
u	$N_x n_x + N_{xy} n_y$
v	$N_{xy} n_x + N_y n_y$
w	$Q_x n_x + Q_y n_y$
u^j	$N_x^j n_x + N_{xy}^j n_y$
v^j	$N_{xy}^j n_x + N_y^j n_y$

(8)

where (n_x,n_y) denote the direction cosines of a unit normal to the boundary of the midplane Ω.

Constitutive Equations

The constitutive equations of an orthotropic lamina in the laminate coordinate system are given by

$$\begin{Bmatrix} \sigma_x \\ \sigma_y \\ \sigma_{xy} \\ \sigma_{yz} \\ \sigma_{xz} \end{Bmatrix}_{(k)} = \begin{bmatrix} Q_{11} & Q_{12} & Q_{16} & 0 & 0 \\ Q_{12} & Q_{22} & Q_{26} & 0 & 0 \\ Q_{16} & Q_{26} & Q_{66} & 0 & 0 \\ 0 & 0 & 0 & Q_{55} & Q_{45} \\ 0 & 0 & 0 & Q_{45} & Q_{44} \end{bmatrix}_{(k)} \begin{Bmatrix} \epsilon_x \\ \epsilon_y \\ 2\epsilon_{xy} \\ 2\epsilon_{xz} \\ 2\epsilon_{yz} \end{Bmatrix}_{(k)} \tag{9}$$

Substitution of Eq. (9) into Eq. (6b) gives the following laminate constitutive equations:

$$\begin{Bmatrix} N_x \\ N_y \\ N_{xy} \\ Q_x \\ Q_y \end{Bmatrix} = \begin{bmatrix} A_{11} & A_{12} & A_{16} & 0 & 0 \\ A_{12} & A_{22} & A_{26} & 0 & 0 \\ A_{16} & A_{26} & A_{66} & 0 & 0 \\ 0 & 0 & 0 & A_{55} & A_{45} \\ 0 & 0 & 0 & A_{45} & A_{44} \end{bmatrix} \times \begin{Bmatrix} \dfrac{\partial u}{\partial x} + \dfrac{1}{2}\left(\dfrac{\partial w}{\partial x}\right)^2 \\ \dfrac{\partial v}{\partial y} + \dfrac{1}{2}\left(\dfrac{\partial w}{\partial y}\right)^2 \\ \dfrac{\partial u}{\partial y} + \dfrac{\partial v}{\partial x} + \dfrac{\partial w}{\partial x}\dfrac{\partial w}{\partial y} \\ \dfrac{\partial w}{\partial x} \\ \dfrac{\partial w}{\partial y} \end{Bmatrix} + \sum_{j=1}^{n} \begin{bmatrix} B_{11}^j & B_{12}^j & B_{16}^j & 0 & 0 \\ B_{22}^j & B_{22}^j & B_{26}^j & 0 & 0 \\ B_{16}^j & B_{26}^j & B_{66}^j & 0 & 0 \\ 0 & 0 & 0 & B_{55} & B_{45}^j \\ 0 & 0 & 0 & B_{45} & B_{44}^j \end{bmatrix} \begin{Bmatrix} \dfrac{\partial u^j}{\partial x} \\ \dfrac{\partial v^j}{\partial y} \\ \dfrac{\partial u^j}{\partial y} + \dfrac{\partial v^j}{\partial x} \\ u^j \\ v^j \end{Bmatrix} \tag{10a}$$

$$\begin{Bmatrix} N_x^j \\ N_y^j \\ N_{xy}^j \\ Q_x^j \\ Q_y^j \end{Bmatrix} = \begin{bmatrix} B_{11}^j & B_{12}^j & B_{16}^j & 0 & 0 \\ B_{12}^j & B_{22}^j & B_{26}^j & 0 & 0 \\ B_{16}^j & B_{26}^j & B_{66}^j & 0 & 0 \\ 0 & 0 & 0 & B_{55}^j & B_{45}^j \\ 0 & 0 & 0 & B_{45}^j & B_{44}^j \end{bmatrix}$$

$$\times \begin{Bmatrix} \dfrac{\partial u}{\partial x} + \dfrac{1}{2}\left(\dfrac{\partial w}{\partial x}\right)^2 \\ \dfrac{\partial v}{\partial y} + \dfrac{1}{2}\left(\dfrac{\partial w}{\partial y}\right)^2 \\ \dfrac{\partial u}{\partial y} + \dfrac{\partial v}{\partial x} + \dfrac{\partial w}{\partial x}\dfrac{\partial w}{\partial y} \\ \dfrac{\partial w}{\partial x} \\ \dfrac{\partial w}{\partial y} \end{Bmatrix}$$

$$+ \sum_{k=1}^{n} \begin{bmatrix} D_{11}^{jk} & D_{12}^{jk} & D_{16}^{jk} & 0 & 0 \\ D_{12}^{jk} & D_{22}^{jk} & D_{26}^{jk} & 0 & 0 \\ D_{16}^{jk} & D_{26}^{jk} & D_{66}^{jk} & 0 & 0 \\ 0 & 0 & 0 & D_{55} & D_{45}^{jk} \\ 0 & 0 & 0 & D_{45} & D_{44}^{jk} \end{bmatrix}$$

$$\times \begin{Bmatrix} \dfrac{\partial u^k}{\partial x} \\ \dfrac{\partial v^k}{\partial y} \\ \dfrac{\partial u^k}{\partial y} + \dfrac{\partial v^k}{\partial y} \\ u^k \\ v^k \end{Bmatrix} \tag{10b}$$

where

$$A_{pq} = \sum_{k=1}^{N} \int_{z_k}^{z_{k+1}} Q_{pq}^{(k)}\, dz \quad (p,q = 1,2,6;4,5)$$

$$B_{pq}^j = \sum_{k=1}^{N} \int_{z_k}^{z_{k+1}} Q_{pq}^{(k)}\, \Phi_j\, dz \quad (p,q = 1,2,6)$$

$$D_{pq}^{ji} = \sum_{k=1}^{N} \int_{z_k}^{z_{k+1}} Q_{pq}^{(k)} \Phi_j \Phi_i\, dz \quad (p,q = 1,2,6)$$

$$B_{pq}^j = \sum_{k=1}^{N} \int_{z_k}^{z_{k+1}} Q_{pq}^{(k)} \frac{d\Phi_j}{dz}\, dz \quad (p,q = 4,5)$$

$$D_{pq}^{ji} = \sum_{k=1}^{N} \int_{z_k}^{z_{k+1}} Q_{pq}^{(k)} \frac{d\Phi_j}{dz} \frac{d\Phi_i}{dz}\, dz \quad (p,q = 4,5) \tag{10c}$$

Finite Element Formulation

The generalized displacements (u,v,w,u^j,v^j) are expressed over each element as a linear combination of the two-dimensional interpolation functions ψ_i and the nodal values $(u_i,v_i,w_i,u_i^j,v_i^j)$ as follows[8]:

$$(u,v,w,u^j,v^j) = \sum_{i=1}^{m} (u_i,v_i,w_i,u_i^j,v_i^j)\psi_i \tag{11}$$

where m is the number of nodes per element. Using Eqs. (3) and (4), the linear components of the strains can be expressed in the form

$$\{\epsilon\} = [B]\{\Delta\}$$

$$\{\epsilon^j\} = [\bar{B}]\{\Delta^j\} \tag{12a}$$

where

$$\{\Delta\}^T = \{u_1,v_1,w_1,\ldots,u_m,v_m,w_m\}$$

$$\{\Delta^j\}^T = \{u_1^j,v_1^j,\ldots,u_m^j,v_m^j\} \tag{12b}$$

Similarly, the nonlinear component of the strains can be written in the form

$$\{\eta\} = [B_{NL}]\{\Delta\} \tag{12c}$$

The matrices $[B]$, $[\bar{B}]$, and $[B_{NL}]$ are given in Appendix A. Using Eqs. (12) in the virtual work statement of Eq. (6a), we obtain

$$\begin{aligned} 0 = \int_\Omega & (\{\delta\Delta\}^T[B]^T[A][B]\{\Delta\} + \{\delta\Delta\}^T[B]^T[A][B_{NL}]\{\Delta\} \\ & + 2\{\delta\Delta\}^T[B_{NL}]^T[A][B]\{\Delta\} + 2\{\delta\Delta\}^T[B_{NL}]^T[A][B_{NL}]\{\Delta\} \\ & + \sum_j^N [\{\delta\Delta\}^T[B]^T[B^j][\bar{B}]\{\Delta^j\} + 2\{\delta\Delta\}^T[B_{NL}]^T[B^j][\bar{B}]\{\Delta^j\} \\ & + \{\delta\Delta^j\}^T[\bar{B}]^T[B^j][B]\{\Delta\} + \{\delta\Delta^j\}^T[\bar{B}]^T[B^j][B_{NL}]\{\Delta\} \\ & + \sum_r^N [\{\delta\Delta^j\}^T[\bar{B}]^T[D^{jr}][\bar{B}]\{\Delta^r\}]] - p\delta w)\, dA \end{aligned}$$

The finite element model is given by

$$\begin{bmatrix} [k^{11}] & [k_1^{12}] & \ldots & [k_N^{12}] \\ [k_1^{21}] & [k_{11}^{22}] & \ldots & . \\ \vdots & & & \vdots \\ [k_N^{21}] & & \ldots & [k_{NN}^{22}] \end{bmatrix} \begin{Bmatrix} \{\Delta\} \\ \{\Delta^1\} \\ \vdots \\ \{\Delta^N\} \end{Bmatrix} = \begin{Bmatrix} \{q\} \\ \{q^1\} \\ \\ \{q^N\} \end{Bmatrix} \tag{13}$$

where the submatrices $[k^{11}]$, $[k_j^{12}]$, $[k_j^{21}]$, $[k_{ji}^{22}]$ with $i,j = 1,\ldots,N$ are given in Appendix B. The load vectors $\{q\}$, $\{q^1\}\ldots\{q^N\}$ are analogous to $\{\Delta\}$, $\{\Delta^1\}$, ... $\{\Delta^N\}$ in Eq. (12b). The nonliner algebraic system is solved by the Newton-Raphson algorithm. The components of the Jacobian matrix are given in Appendix B.

The in-plane components of the stresses $(\sigma_x,\sigma_y,\sigma_{xy})$ and their inplane derivatives $(\sigma_{x,x};\ \sigma_{y,y};\ \sigma_{xy,z};\ \sigma_{xy,y})$ are computed from the constitutive equations for each layer, i.e.,

$$\begin{Bmatrix} \sigma_x \\ \sigma_y \\ \sigma_{xy} \end{Bmatrix} = \begin{bmatrix} Q_{11} & Q_{12} & Q_{13} \\ Q_{12} & Q_{22} & Q_{23} \\ Q_{13} & Q_{23} & Q_{33} \end{bmatrix}$$

$$\times \begin{Bmatrix} \dfrac{\partial u}{\partial x} + \dfrac{1}{2}\left(\dfrac{\partial w}{\partial x}\right)^2 + \sum_{j=1}^{N} \dfrac{\partial u^j}{\partial x}\psi_j \\ \dfrac{\partial v}{\partial y} + \dfrac{1}{2}\left(\dfrac{\partial w}{\partial y}\right)^2 + \sum_{j=1}^{N} \dfrac{\partial v^j}{\partial y}\psi_j \\ \dfrac{\partial u}{\partial y} + \dfrac{\partial v}{\partial x} + \dfrac{\partial w}{\partial x}\dfrac{\partial w}{\partial y} + \sum_{j=1}^{N}\left(\dfrac{\partial u^j}{\partial y} + \dfrac{\partial v^j}{\partial x}\right)\psi_j \end{Bmatrix} \tag{14}$$

Next, the interlaminar shear stresses (σ_{xz} and σ_{yz}) are recovered[6] from the equilibrium equations

$$\sigma_{xz,z} = -(\sigma_{x,x} + \sigma_{xy,y})$$

$$\sigma_{yz,z} = -(\sigma_{xy,x} + \sigma_{y,y}) \tag{15}$$

The nonlinear equations are also linearized to formulate the eigenvalue problem associated with bifurcation (buckling) analysis,

$$([K_D] - \lambda[K_G]) \cdot \Phi = 0 \tag{16}$$

where $[K_D]$ is the linear part of the direct stiffness matrix (13), and $[K_G]$ is the geometric stiffness matrix obtained from the nonlinear part of Eq. (13) by perturbation of the nonlinear equations around the equilibrium position.[13]

Numerical Examples

The first couple of sample problems are intended to validate the nonlinear finite element model developed herein. The problems of composite laminates are selected to illustrate certain aspects of the solution that are not often seen in isotropic plates or even symmetric laminates.

Clamped Isotropic ($\nu = 0.3$) Plate

Consider a clamped square plate of side $a = 1000$ mm, thickness $h = 2$ mm, and subjected to uniformly distributed transverse load $p = \lambda p_0$ ($p_0 = 100\ \text{N/m}^2$). Figure 1 shows the variation of σ_{xx}/p at the top, bottom, and middle surface of the plate as a function of the load parameter λ. A 2×2 mesh of nine-node quadratic elements is used in a quarter plate. The stress is obtained at the Gauss point, $x = 0.973a$, $y = 0.527a$. It is clear that the effect of the geometric nonlinearity is to reduce the maximum stress from the value predicted by the linear theory. As can be seen from Fig. 1, the membrane effects dominate over the bending effects as the load is increased. The linear theory overestimates the stress at the surface and underestimates it at the middle surface. Composite materials, usually stronger in tension than in shear, can be used more efficiently in situations where membrane forces are significant.

Figure 2 contains the transverse deflection as a function of the load parameter, which compares well with that of Ref. 10. For isotropic plates, the distribution of stresses and displacements through the thickness is linear, as shown in Fig. 3. The maximum stress, at the surface of the plate, is due to bending. The effect of the nonlinearity is to reduce the value of stress at the top and bottom surfaces and to increase it at the middle surface of the plate. The stress results presented in Fig. 3 correspond to the point: $x = 0.973a$, $y = 0.527a$.

Cross-Ply [0/90] Simply Supported Plate under Uniform Load

A simply supported cross-ply [0/90] laminate under uniform transverse load is analyzed. The geometry used is the same as in the preceding example. The following material properties and boundary conditions are used:

$$E_1 = 250\ \text{GPa},\ E_2 = 20\ \text{GPa},\ G_{12} = G_{13} = 10\ \text{GPa}$$

$$G_{23} = 4\ \text{GPa},\ \nu_{12} = 0.25$$

$$v = w = \phi_2 = 0 \text{ at } x = a/2$$

$$u = w = \phi_1 = 0 \text{ at } y = a/2$$

$$u = \phi_1 = 0 \text{ at } x = 0$$

$$v = \phi_2 = 0 \text{ at } y = 0 \tag{17}$$

where $\phi_1(x,y)$ and $\phi_2(x,y)$ are the rotations about the y and x axes, respectively. These rotations can be expressed in terms of the u^j and v^j at the nodes. For example, $\phi_2(x,y) = 0$ is satisfied by setting all $v^j = 0$ through the thickness at that (x,y) location.

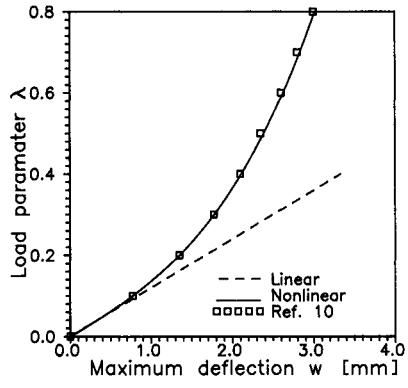

Fig. 2 Load-deflection curve for a clamped isotropic plate under transverse load; results from GLPT compared to those of Ref. 10.

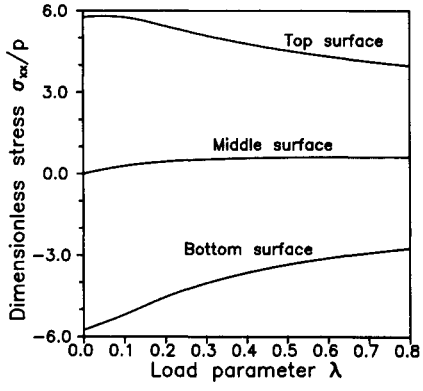

Fig. 1 Maximum stress as a function of the load for a clamped isotropic plate under uniformly distributed transverse load shows the stress relaxation as the membrane effect becomes dominant.

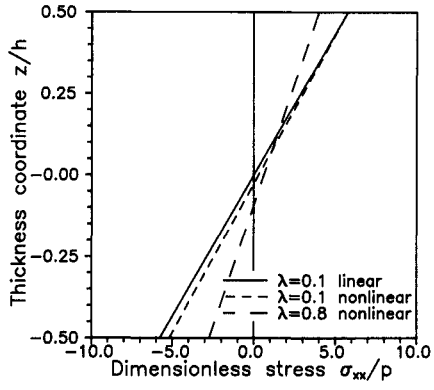

Fig. 3 Distribution of the in-plane normal stress σ_{xx} for a clamped isotropic plate under transverse load for several values of the load showing the stress relaxation as the load increases.

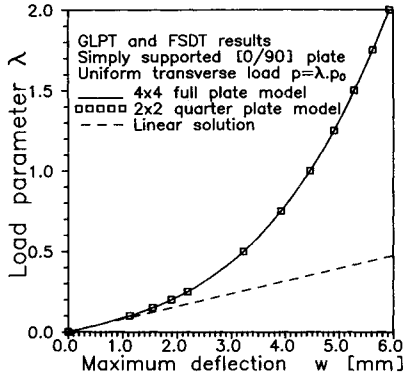

Fig. 4 Simply supported cross-ply [0/90] plate under transverse load; both theories, GLPT and FSDT, and both models, 2 × 2 quarter plate and 4 × 4 full plate, produce the same transverse deflections.

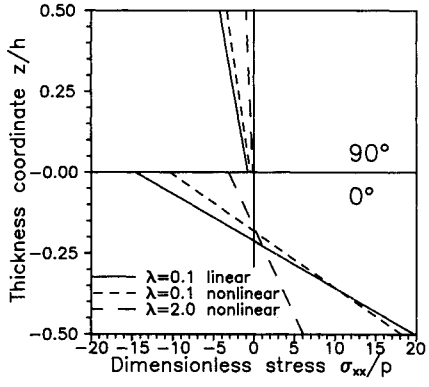

Fig. 5 Through the thickness distribution of the in-plane normal stress σ_{xx} for a simply supported cross-ply [0/90] plate for several values of the load.

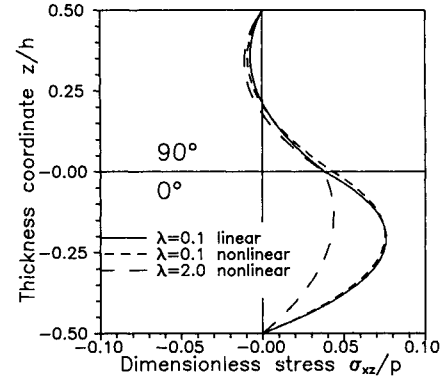

Fig. 6 Through the thickness distribution of the in-plane normal stress σ_{xx} for a simply supported cross-ply [0/90] plate for several values of the load.

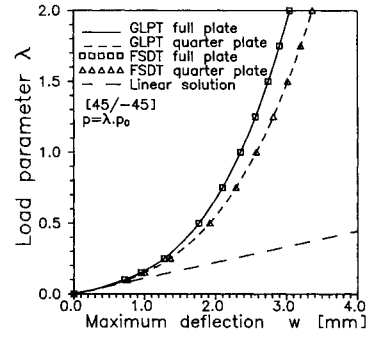

Fig. 7 Load-deflection curves for a simply supported angle-ply [45/−45] plate under transverse load, obtained from a 2 × 2 quarter-plate model and a 4 × 4 full-plate model using GLPT and FSDT.

In order to investigate the effect of the symmetry boundary conditions, results on both a 2 × 2 quarter-plate and a 4 × 4 full-plate model are reported in Fig. 4. For cross-ply plates, the symmetry boundary conditions used in the quarter-plate model are found to be identical to the corresponding values obtained from the full-plate model. Therefore, the maximum transverse deflections as a function of the load parameter λ, shown in Fig. 4, are identical for both models. This turns out not to be the case for angle-ply laminates as we shall see in the next example. Note that both the first-order shear deformation theory (FSDT) and the generalized laminated plate theory (GLPT) predict identical values of the transverse deflection w in Fig. 4 because the shear deformation effects are negligible for the thickness ratio ($a/h = 500$) considered in this example. The distribution of the in-plane normal stress σ_{xx} at $x = y = 0.526a$ is shown in Fig. 5, and the distribution of the interlaminar shear stress σ_{xz} at $x = 0.973a$, $y = 0.526a$ is shown in Fig. 6. The values of stresses reduce with the increasing load. The reduction of interlaminar stresses is of definite significance for composite materials, usually stronger in tension than in shear.

Simply Supported Angle-Ply [45/ − 45] Plate under Uniform Load

In order to investigate the effect of the symmetry boundary conditions for angle-ply laminates, we consider a 2 × 2 mesh to model a quarter of a plate and a 4 × 4 mesh to model the full plate. The nine-node quadratic element is used. The material properties, load, and geometry are the same as in the preceding example. Load-deflection curves obtained from both models are shown in Fig. 7. A discrepancy between the load-deflection curves of the two models is observed; the full model is more rigid. In order to explain this discrepancy, it must be noted that the symmetry boundary conditions used in the quarter-plate model were derived[11] using the exact solution to the linear problem formulated in terms of the FSDT. For the angle-ply case, the assumed GLPT solution is

$$u = U \sin\frac{x\pi}{a}\cos\frac{y\pi}{b}$$

$$v = V \cos\frac{x\pi}{a}\sin\frac{y\pi}{b}$$

$$w = W \sin\frac{x\pi}{a}\sin\frac{y\pi}{b}$$

$$v^j = V^j \cos\frac{x\pi}{a}\sin\frac{y\pi}{b}$$

$$u^j = U^j \sin\frac{x\pi}{a}\cos\frac{y\pi}{b} \tag{18}$$

which satisfies both the displacement and stress symmetry boundary conditions at the centerlines ($x = a/2$ and $y = b/2$) of the plate for the linear case:

$$v(a/2,y) = u^j(a/2,y) = 0; \quad N_1(a/2,y) = N_2^j(a/2,y) = 0$$

$$u(x,b/2) = v^j(x,b/2) = 0; \quad N_2(x,b/2) = N_1^j(x,b/2) = 0 \tag{19}$$

However, once the nonlinear terms are incorporated into the stress resultants of Eq. (10a), the force boundary conditions are no longer satisfied:

$$N_1(a/2,y) = A_{12}\frac{\pi^2 w^2}{2b^2}\cos^2(y\pi/b) \neq 0$$

$$N_2(x,b/2) = A_{12}\frac{\pi^2 w^2}{2a^2}\cos^2(y\pi/a) \neq 0 \tag{20}$$

Since the force boundary conditions are automatically set to zero in a finite element model in which corresponding displacements are not specified, the problem solved is not the one in which Eq. (20) is valid. Since a plate with nonzero in-plane forces is stiffer than with zero in-plane forces, the associated transverse deflections will be different with the quarter-plate model yielding larger deflections. Note that the transverse deflections predicted by GLPT compare very well with FSDT in Fig. 7.

It can be shown that the normal to the middle plane does not remain straight after deformation, as is assumed in FSDT. The distribution of in-plane displacements of the point $x = 0$, $y = 3a/4$ (relative to the middle surface displacement) through the thickness of the laminate is shown in Fig. 8. With increasing load, the bending effect reduces and so also the departure of the distribution of in-plane displacements from a straight line.

Hybrid Composite Laminates

This example is included to compare the prediction of interlaminar shear stress obtained with the FSDT and the GLPT presented in this work. Consider a five-layer laminated plate composed of aluminum and Aramid layers. Each aluminum layer is 0.03048 mm thick, and each Aramid layer is 0.0288 mm thick (see Fig. 9). The plate is simply supported and subjected to a uniformly distributed transverse load. The distribution through the thickness of $\bar{\sigma}_{yz} = [(h/p_0\, a)]\ \sigma_{yz}$ is shown in Fig. 9.

The FSDT assumes a constant value of the shear strain γ_{yz} through the entire thickness of the plate. Consequently, FSDT produces a layer-wise constant value of σ_{yz} predicting a low value of σ_{yz} in the Aramid layers due to their small shear modulus and to the fact that the shear strain is small due to the effect of the aluminum layers that contribute to the averaged shear stiffness of the plate with their high shear modulus.

The GLPT assumes a constant value of the shear strain λ_{yz} on each individual layer. Consequently, GLPT predicts large shear strains in the Aramid layers that lead to the correct value of the shear stress σ_{yz} as shown by solid lines in Fig. 9. The integration of the equilibrium equations[5,6] that takes into account the layer-wise constant value of σ_{yz} produces a parabolic distribution of σ_{yz} on each layer as shown in Fig. 9. Further comparisons of interlaminar stress distributions with three-dimensional elasticity solutions and various plate theories can be found in Refs. 5, 6, and 13.

Buckling and Postbuckling of Angle-Ply [45/−45] and Cross-Ply [0/90] Laminates under In-Plane Load

A plate with $a = b = 1000$ mm, $h = 2$ mm is used to analyze a [45/−45] simply supported laminate under uniform in-plane compressive load $N_y = \lambda N_{y0}$ ($N_{y0} = 10.85$ N/m). The material properties used are $E_1/E_2 = 40$; $E_2 = 6.25$ GPa; $G_{12}/E_2 = 0.82$; $G_{13} = G_{12}$; $G_{23}/E_2 = 0.52$; $\nu_{12} = 0.24$. Although an exact solution of the eigenvalue problem associated with the buckling equations exists for this case,[12] the boundary conditions used to obtain that solution cannot be used for the nonlinear analysis. For the nonlinear analysis, the boundary conditions have to allow an applied load, $N_x = 0$ and $N_y = \lambda N_{y0}$. The nonlinear response is shown in Fig. 10, normalized with respect to the critical load obtained by an analytical solution. It is evident that the nonlinear analysis estimates the critical load accurately. An excellent correlation between GLPT- and FSDT-predicted deflections is observed.

The eigenvalue problem, which leads to an accurate prediction of the critical load for laminates without bending-extension coupling, is formulated with the assumption that prebuckling deformations do not include nonzero transverse deflections. This assumption is not satisfied in the next example.

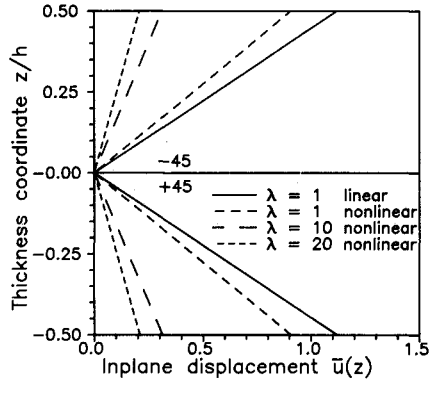

Fig. 8 In-plane displacements $\bar{u}(z) = [u(z) - u_0]0.20/v_{max}$, at $x = a/2$, $y = 3b/4$ for a [45/−45] laminated plate under uniformly distributed transverse load, where u_0 is the middle surface displacement.

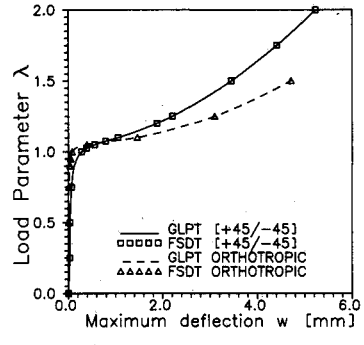

Fig. 10 Load-deflection curves for angle-ply [45/−45] and orthotropic simply supported plates under in-plane load N_y.

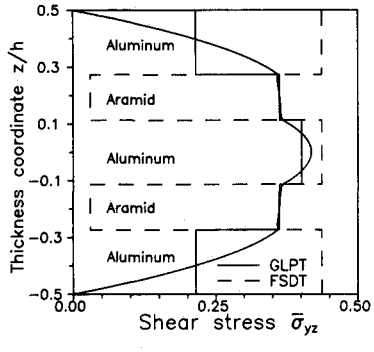

Fig. 9 Through the thickness distribution of the interlaminar stress $\bar{\sigma}_{yz} = [(h/p_0 a)]\sigma_{yz}$ in a simply supported plate under uniformly distributed transverse load p_0.

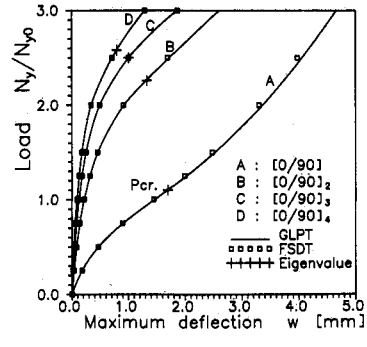

Fig. 11 Antisymmetric cross-ply simply supported, subjected to in-plane load N_y; the critical loads from a closed form solution (eigenvalues) are shown on the corresponding load-deflection curves.

An antisymmetric cross-ply laminate under in-plane load $N_y = \lambda N_{y0}$ ($N_{y0} = 6.25$ N/m) is considered next. In this case the prebuckling transverse deflections are important. The geometry and material properties are the same as in the preceding example. The simply supported boundary conditions of cross-ply laminates [see Eq. (17) and SS-1 in Ref. 11] are used for the 4 × 4 full-plate model (although the 2 × 2 mesh in a quarter plate would be all right in this case). In order to assess the effect of the number of layers, four laminates are analyzed as shown in Fig. 11 where [0/90] is a two-layer laminate, $[0/90]_2$ is a four-layer laminate, etc. The values of the critical buckling load given by the exact solution of the eigenvalue problem[12] are depicted on the corresponding load-deflection curves for comparison. It is evident that in this case the eigenvalues are not representative of any bifurcation points of the structure. The structure behaves nonlinearly for all values of the load.[13]

Conclusions

The nonlinear version of the GLPT and its associated finite element models are developed. The GLPT proves to be an accurate theory for the nonlinear analysis of laminated composite plates. It provides the correct global response and highly accurate prediction of stress distributions, which are of paramount importance for the assessment of damage and life of composite structures. The model is validated with a variety of examples that also serve to highlight certain interesting features of certain laminated composite plates. The effect of symmetry boundary conditions on the nonlinear analysis and the effect of bending extension coupling on the buckling analysis of laminated plates are also investigated. Stress relaxation due to nonlinear effects is shown to be an important factor in the design of composite plates. An extension of this theory to model buckling of delaminated plates is reported in Ref. 13.

Appendix A: Strain-Displacement Matrices

The strains $\{e\}$, $\{\eta\}$, and $\{e^j\}$ appearing in Eqs. (12) are

$$\{e\} = \begin{Bmatrix} \dfrac{\partial u}{\partial x} \\ \dfrac{\partial v}{\partial y} \\ \dfrac{\partial u}{\partial y} + \dfrac{\partial v}{\partial x} \\ \dfrac{\partial w}{\partial x} \\ \dfrac{\partial w}{\partial y} \end{Bmatrix}, \quad \{e^j\} = \begin{Bmatrix} \dfrac{\partial u^j}{\partial x} \\ \dfrac{\partial v^j}{\partial y} \\ \dfrac{\partial u^j}{\partial y} + \dfrac{\partial v^j}{\partial x} \\ u^j \\ v^j \end{Bmatrix}$$

$$\{\eta\} = \begin{Bmatrix} \frac{1}{2}\left(\dfrac{\partial w}{\partial x}\right)^2 \\ \frac{1}{2}\left(\dfrac{\partial w}{\partial y}\right)^2 \\ \dfrac{\partial w}{\partial x}\dfrac{\partial w}{\partial y} \\ 0 \\ 0 \end{Bmatrix}$$

The matrices $[B]$, $[\bar{B}]$, and $[B_{NL}]$ appearing in the strain-displacement relations of Eqs. (12) are

$$[B] = \begin{bmatrix} \dfrac{\partial \psi_i}{\partial x} & 0 & 0 \\ 0 & \dfrac{\partial \psi_i}{\partial y} & 0 \\ \dfrac{\partial \psi_i}{\partial y} & \dfrac{\partial \psi_i}{\partial x} & 0 \\ 0 & 0 & \dfrac{\partial \psi_i}{\partial x} \\ 0 & 0 & \dfrac{\partial \psi_i}{\partial y} \end{bmatrix} \quad (5 \times 3 \text{ m})$$

$$[\bar{B}] = \begin{bmatrix} \dfrac{\partial \psi_i}{\partial x} & 0 \\ 0 & \dfrac{\partial \psi_i}{\partial y} \\ \dfrac{\partial \psi_i}{\partial y} & \dfrac{\partial \psi_i}{\partial x} \\ \psi_i & 0 \\ 0 & \psi_i \end{bmatrix} \quad (5 \times 2 \text{ m})$$

$$[B_{NL}] = \frac{1}{2} \begin{bmatrix} 0 & 0 & \dfrac{\partial w}{\partial x}\dfrac{\partial \psi_i}{\partial x} \\ 0 & 0 & \dfrac{\partial w}{\partial y}\dfrac{\partial \psi_i}{\partial y} \\ 0 & 0 & \dfrac{\partial w}{\partial x}\dfrac{\partial \psi_i}{\partial y} + \dfrac{\partial w}{\partial y}\dfrac{\partial \psi_i}{\partial x} \\ 0 & 0 & 0 \\ 0 & 0 & 0 \end{bmatrix} \quad (5 \times 3 \text{ m})$$

with $(i = 1, \ldots, m)$.

Appendix B: Stiffness Matrices

$$[k^{11}] = \int_\Omega ([B]^T[A][B] + [B]^T[A][B_{NL}] + 2[B_{NL}]^T[A][B] + 2[B_{NL}]^T[A][B_{NL}])d\Omega$$

$$[k_j^{12}] = \int_\Omega ([B]^T[B^j][\bar{B}] + 2[B_{NL}]^T[B^j][\bar{B}])d\Omega$$

$$[k_j^{21}] = \int_\Omega ([\bar{B}]^T[B^j][B] + [\bar{B}]^T[B^j][B_{NL}])d\Omega$$

$$[k_{jr}^{22}] = \int_\Omega ([\bar{B}]^T[D^{jr}][\bar{B}])d\Omega$$

The Jacobian matrix is

$$[J] = \begin{bmatrix} \left[\frac{\partial\{R^0\}}{\partial\{\Delta\}}\right] & \left[\frac{\partial\{R^0\}}{\partial\{\Delta^1\}}\right] & \cdots & \left[\frac{\partial\{R^0\}}{\{\partial\Delta^N\}}\right] \\ \left[\frac{\partial\{R^1\}}{\partial\{\Delta\}}\right] & \left[\frac{\partial\{R^1\}}{\partial\{\Delta^1\}}\right] & \cdots & \left[\frac{\partial\{R^1\}}{\{\partial\Delta^N\}}\right] \\ \vdots & \vdots & \cdots & \vdots \\ \left[\frac{\partial\{R^N\}}{\partial\{\Delta\}}\right] & \left[\frac{\partial\{R^N\}}{\partial\{\Delta^1\}}\right] & \cdots & \left[\frac{\partial\{R^N\}}{\{\partial\Delta^N\}}\right] \end{bmatrix}$$

where

$$\{R^0\} = [k^{11}]\{\Delta\} + \sum_{j}^{N} [k_j^{12}]\{\Delta^j\}$$

$$\{R^j\} = [k_j^{12}]\{\Delta\} + \sum_{r}^{N} [k_{jr}^{22}]\{\Delta^r\};\ (j = 1,\ldots, N)$$

References

[1]Reddy, J. N., *Energy and Variational Methods in Applied Mechanics,* Wiley, New York, 1984.

[2]Reddy, J. N., "A Generalization of Two-Dimensional Theories of Laminated Composite Plates," *Commun. Applied Numer. Methods,* Vol. 3, 1987, pp. 113–180.

[3]Srinivas, S., "A Refined Analysis of Composite Lamintes," *Journal of Sound and Vibration,* Vol. 30, No. 4, 1973, pp. 495–507.

[4]Hinrichsen, R. L., and Palazotto, A. N., "The Nonlinear Finite Element Analysis of Thick Composite Plates Using a Cubic Spline Function," *AIAA Journal,* Vol. 24, No. 11, 1986, pp. 1836–1842.

[5]Barbero, E. J. Reddy, J. N., and Teply, J. L., "An Accurate Determination of Stresses in Thick Laminates Using a Generalized Plate Theory," *International Journal of Numerical Methods in Engineering,* Vol. 28, 1989, pp. 1–14.

[6]Reddy, J. N., Barbero, E. J., and Teply, J. L., "A Plate Bending Element Based on a Generalized Laminate Plate Theory," *International Journal of Numerical Methods in Engineering,* Vol. 28, 1989, pp. 2275–2292.

[7]Barbero, E. J., and Reddy, J. N., "A General Two-Dimensional Theory of Laminated Cylindrical Shells," *AIAA Journal* (to be published).

[8]Reddy, J. N., *An introduction to the Finite Element Method,* McGraw-Hill, New York, 1984.

[9]Reddy, J. N. "A Simple Higher-Order Theory for Laminated Composite Plates," *Journal of Applied Mechanics,* Vol. 51, 1984, pp. 745–752.

[10]Way, S., "A Laterally Loaded Clamped Square Plate with Large Deformation," *Proceedings of the 5th International Conference on Applied Mechanics,* Wiley, New York, 1938, pp. 123–138.

[11]Reddy, J. N. "A Note on Symmetry Considerations in the Transient Response of Unsymmetrically Laminated Anisotropic Plates," *International Journal of Numerical Methods in Engineering,* Vol. 20, 1984, pp. 175–194.

[12]Jones, R. M., *Mechanics of Composite Materials,* Scripta Book Co., Washington, DC, 1975.

[13]Barbero, E. J., "On a Generalized Laminated Plate Theory with Application to Bending Vibration and Delamination Buckling," Ph.D. Dissertation, Virginia Polytechnic Institute and State University, Blacksburg, VA, Oct. 1989.